Spine

SPINE Volume 36, Number 6, pp E373–E379

BASIC SCIENCE

Autologous Stem Cell Therapy Maintains Vertebral Blood Flow and Contrast Diffusion Through the Endplate in Experimental Intervertebral Disc Degeneration

Michael Bendtsen, PhD,* Cody Eric Bünger, DMSc,* Xuenong Zou, PhD,* Casper Foldager, MS,* and Hans Stødkilde Jørgensen, DMSc†

Study Design. Experimental, controlled, randomized, and paired study.

Objective. To evaluate regenerative effect of stem cell therapy on the vertebral endplate and introduce dynamic contrast-enhanced magnetic resonance imaging (MRI) as a tool in the investigation of endplate function.

Summary of Background Data. The vertebral endplate plays a crucial role in nutritional supply to the intervertebral disc. Estimation of endplate function is an important parameter in future biologic therapy of intervertebral disc degeneration (IDD).

Methods. Four-level IDD was induced in each of 15 Gottingen minipigs. Percutaneous intradiscal injection of two hydrogels (Zimmer Biologics Inc, Austin, TX) and one loaded with stem cells was used as single interventions after 12 weeks. Total observation time was 24 weeks. MRI was performed before the initiation of treatment and killing of animals.

Results. Three animals were excluded because of spondylodiscitis. Stem cell and hydrogel treatment had significantly higher T2 values, relative vertebral blood flow and volume, as well as lower Pfirrmann scores when compared with degenerative controls. No statistical differences were found compared to normal controls.

Conclusion. Stem cell and hydrogel therapy is able to partly regenerate IDD and maintain perfusion and permeability of the vertebral endplate and subchondral bone. Dynamic contrast-enhanced MRI may become an important tool in future investigation of the vertebral endplate.

Key words: intervertebral disc degeneration, mesenchymal stem cells, endplate, DCE-MRI, postcontrast MRI. **Spine 2011;36:E373–E379**

Intervertebral disc degeneration (IDD) is one of the most common low back pain (LBP), which causes disability in adults younger than 45 years, and consequently one of the main reasons for early retirement and low quality of life in industrialized societies.[1]

LBP affects approximately 75% of the population at least once during their life. Ninety percent of patients with LBP recover within 3 months. However, a substantial number of patients do not recover and progress to chronic LBP.

Several surgical procedures have been developed in the treatment of LBP and IDD. Yet, none of the procedures offer physiologic approach but only treat symptoms of IDD. When this is said, the same disc morphology can be seen in asymptomatic individuals. Adequate nutritional supply to the disc is considered an important part not only in the prevention of IDD[2] but also on the success of biologic therapies that have emerged.

In IDD, there is loss of cells, lowering of oxygen tension, and increased levels of lactate-reducing cell metabolism.[3] A decrease in proteoglycans and increased collagen content with subsequent alterations in viscoelastic property shifts loading of the vertebral endplate. This might be the reason to the observed changes in the vertebral endplate seen in IDD. These consist of cracks detectable by various methodologies,[4–6] occlusion of vertebral marrow contact channels,[7] decreased vascularity, and increased bone content.[8]

Nutrient diffusion through the vertebral endplate into the disc depends on fluid flow—into the disc at bed rest and out of the disc during loading—a decrease in permeability because of calcification, marrow channel occlusion, *etc.*, will diminish nutrient transport and affect disc cell metabolism.[9,10]

From the *Orthopeadic Research Laboratory, Aarhus University Hospital, Aarhus, Denmark; and †MR-Research Center, Aarhus University Hospital, Skejby, Denmark.

Acknowledgment date: October 2, 2009. First revision date: December 21, 2009. Second revision date: February 12, 2010. Acceptance date: February 18, 2010.

The legal regulatory status of the device(s)/drug(s) that is/are the subject of this manuscript is not applicable in my country.

Corporate/Industry funds were received in support of this work. Although one or more of the author(s) has/have received or will receive benefits for personal or professional use from a commercial party related directly or indirectly to the subject of this manuscript, benefits will be directed solely to a research fund, foundation, educational institution, or other nonprofit organization which the author(s) has/have been associated.

Supported by Zimmer Biologics Inc, Austin, TX.

Address correspondence and reprint requests to Michael Bendtsen, PhD, Orthopeadic Research Laboratory, Aarhus University Hospital, Aarhus Sygehus, Norrebrogade 44 Building 1A 1, 8000 Aarhus C, Denmark; E-mail: michael.bendtsen@ki.au.dk

DOI: 10.1097/BRS.0b013e3181dce34c

Rajasekaran *et al*[11] established a grading score for the vertebral endplate on the basis of serial postcontrast magnetic resonance imaging (MRI). Diffusion patterns, enhancement percentage, time to peak enhancement, and time intensity curves are summarized in a total endplate score. A significant correlation between total endplate score and IDD was found.[11] However, this is a very time-consuming method that requires six MRIs within 12 hours.

Dynamic contrast-enhanced MRI (DCE-MRI) has been used to investigate blood flow in vertebrae of osteoporotic patients[12] and patients suffering from Paget disease (a rare chronic disorder with increased bone turnover and described in 1877 by Sir James Paget).[13] T1-weighted DCE-MRI allows for calculation of relative perfusion, relative blood volume (rBV) (%), and permeability parameters when fitted to a two-compartmental model. Acquisition is fast (less than 5 minutes) but depends on postprocessing, which can be a little time-consuming (10–15 minutes).

Permeability calculations correlate to angiogenesis and expression of vascular endothelial growth factor, which are believed to be the most potent vascular growth factor and regulator of vascular permeability.[14,15] Intervertebral disc cells constitute only 1% of the volume of the adult disc but their role in maintaining matrix turnover, morphology, and metabolism is crucial.

Recent evidence suggests that disc cells do not undergo apoptosis or necrosis but go into a state of cell hibernation, senescence, from which they might be activated by appropriate stimuli.[16,17] This is supported by evidence of regenerative capacity of transplanted cells—both bone marrow-derived and fat-derived mesenchymal stem cells (MSCs) and autologous disc cells—to degenerative intervertebral discs.

With this in mind, we hypothesized the following: (1) autologous MSC treatment augments the effect of stand-alone hydrogel injection to the nucleus pulposus (NP), (2) regenerative therapies for the NP "protects" the vertebral endplate, and (3) DCE-MRI is a valuable tool in the assessment of endplate function. The aims of this study were—thus in an established Gottingen minipig model—to analyze the effect of MSC treatment on disc degeneration and vertebral endplate function.

MATERIALS AND METHODS

Study Design

Fifteen skeletally mature Gottingen minipigs were used for the study (3–4 years of age and weighing approximately 40 kg). The study was conducted in two parts with six (pilot study) and nine pigs in each. This was because of contaminated hydrogels in the pilot study. Subsequently, the study was expanded to 15 animals.

Surgery

IDD was induced in four levels (L2/L3–L5/L6) by full-thickness scalpel incisions in the left anterolateral annulus fibrosus (blade number 23). Twelve weeks after surgery, induced degenerative levels were randomized for three different treatments and a degenerative control.

A left-sided retroperitoneal approach was used to expose the lumbar spine. The psoas muscle was lifted gently from the intervertebral discs, while muscle attachment to the vertebral body was kept intact and incisions were performed. Hemostasis was secured and the abdomen closed in layers. All animals were neurologically intact and thrived during the observation period.

METHODOLOGY

Autologous bone marrow was aspirated from the proximal tibia into a 50-mL syringe containing 10-mL Dulbecco's Modified Eagle Medium with 50 IE Heparin. A total of 10 mL of bone marrow was aspirated from each animal.

MSCs were purified by Ficoll gradient centrifugation followed by proliferation till passage 2. MSCs were marked intracellularly with quantum dots (QTracker, Invitrogen, Taastrup, Denmark) as described by the manufacturer and kept frozen in liquid nitrogen suspended in Dulbecco's Modified Eagle Medium with 10% DMSO.

Treatment was intradiscal injection of two different hydrogels designated Hydrogel PhotoFix (PF) and Hyaluronic Acid (HA) (Zimmer Biologics Inc, Austin, TX) and 125,000 autologous MSCs suspended in hydrogel PF.

Injections were performed percutaneously with 18-gauge needles. Fluoroscopy was used to verify intradiscal placement in two planes. Hydrogel (0.2 mL) was injected into each disc and pressure maintained for 5 minutes. The needle was retracted to the annulus fibrosus and kept for 2 minutes before removal. Animals were killed 12 weeks after treatment.

EVALUATION

MRI was performed before treatment and killing. MRI consisted of T1-sagittal (repetition time [TR]: 400 milliseconds; echo time [TE]: 14 milliseconds; number of excitations [NEX] 3: 512 × 256), T2-sagittal and axial (TR: 6660 milliseconds; TE: 100 milliseconds; NEX 2: 512 × 256), T2 sagittal mapping (TR: 6660 milliseconds; TE: 15, 50, 85, and 125 milliseconds; NEX 2: 512 × 256), T1-dynamic contrast-enhanced (TR: 1000 milliseconds; TE: 15, 7 milliseconds; Flip angle 15°, 128 × 128; slice thickness 7 mm, three slices, 174 acquisitions). Manual injection of 0.1 mmol/kg gadobenic acid (MultiHance, Bracco, Italy), injection rate of 2 mL/s, and flushed with 20-mL saline immediately after, and T1-sagittal postcontrast after 45 minutes (TR: 400 milliseconds; TE: 14 milliseconds; NEX 3: 512 × 256) sequences. MRI was performed on a clinical 1.5-T GE scanner (GE Signa Excite, Milwaukee, WI). Midsagittal T2 images were graded according to Pfirrmann *et al*.[18]

T2 mapping was performed on an online workstation, whereas perfusion and permeability calculations were performed on an offline PC running DPTools software (Denis Ducreux, MD, PhD, Service de Neuroradiologie Diagnostique, et Thérapeutique, CHU Bicêtre, France). Region of interest was placed in the endplate and subchondral bone.

Contrast enhancement was calculated by the following formula:

$$\text{Enhancement (\%)} = (SI_{pre} - SI_{post})/SI_{pre} \times 100$$

where SI is signal intensity.

Spines of the animals were removed *en bloc* after killing, flash frozen in liquid nitrogen, and stored at −80°C. Spines were cut into motion segments and split in the midsagittal plane. Confocal laser microscopy (Zeiss LSM 510) was performed on the blocks after counterstaining with DAPI (4′, 6 Diamidino-2-phenylindoledidihydrochloride). The blocks were dehydrated in graded series of alcohol and embedded in cold methyl methacrylate and sectioned (7 μm) on a Leiden microtome.

Ethics

The study was approved by the Animal Welfare Committee.

RESULTS

In the first study (pilot with six animals), three of the animals were excluded because of spondylodiscitis. On killing animals, samples were taken from the infected discs and sent for determination of the bacterial species. At the same time, samples from the injected hydrogel were analyzed. In all infected levels and corresponding hydrogels, growth of *Staphylococcus aureus* was found. Serotyping was not performed.

In all levels treated with hydrogel PF and autologous stem cells, quantum dot-labeled cells were found (Figure 1). Labeled cells appeared with a blue nuclei (DAPI) surrounded by green dots (QTracker). Therefore, transplanted stem cells were found to be alive after 12 weeks *in vivo*.

Before randomization for treatment or degenerative control, levels were Pfirrmann grade 2 to 3. Twelve weeks posttreatment, levels treated with stem cells and hydrogel PF were grade 2.1, and hydrogel PF 2.8, hydrogel HA 2.9, and degenerative controls deteriorated to grade 3.5. Normal controls continued to be grade 1.

Pre- and posttreatment T2-sagittal images are presented in Figure 2. On T2 mapping, normal control levels had a relaxation time at 94.4 ± 4.3 milliseconds. Levels treated with stem cells and hydrogel PF had 87.6 ± 5.9 milliseconds. Hydrogel PF and Hydrogel HA had relaxation times of 73.1 ± 5.4 and 68.9 ± 4.6 milliseconds, respectively, whereas degenerative controls had a relaxation time of 61.7 ± 5.9 milliseconds. Normal controls, stem cells-hydrogel PF, and hydrogel PF had significantly higher relaxation times than degenerative controls ($P < 0.0001$, $P < 0.0001$, $P < 0.0001$, and $P = 0.0006$). Stem cells-hydrogel PF had higher values than hydrogels alone ($P < 0.0001$, $P = 0.0003$), but not statistically different from normal controls ($P = 0.07$).

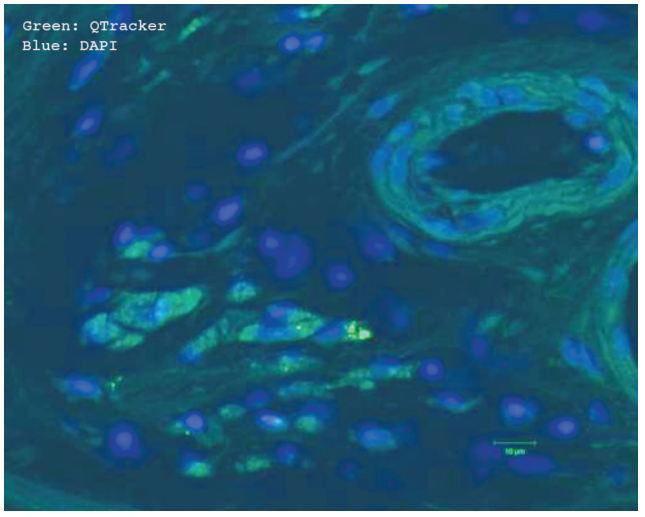

Figure 1. Confocal microscopy—nuclei is stained blue (DAPI), while QTracker stains green with placement in cytoplasma around blue nuclei. Bar is 10 μm.

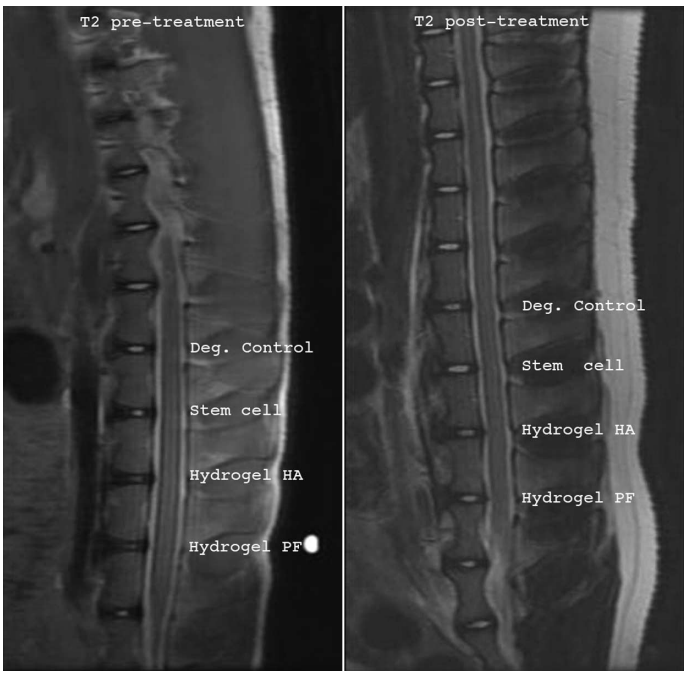

Figure 2. T2-midsagittal images. Left side is before interventions. Right side is 12 weeks after treatment. Stem cell-hydrogel has gained signal intensity (SI) and size. Nucleus pulposus is homogeneous. Degenerate control is smaller and with lower SI, inhomogeneous signal. Two hydrogels have gained some SI and appear a little larger.

The discs were easily identifiable on T2 maps, irrespective of Pfirrmann grade. Discs were uniform in color coding. No visual change in color was observed from the periphery to the center of the NP in any discs. Normal discs had a green to blue NP. There was a color shift toward green to yellow with the degenerative grade.

Representative T2 maps of the same animal as shown in Figure 2 are shown in Figure 3, whereas data are summarized in Table 1. There was a significant difference in relative blood flow (rBF) and rBV between normal and degenerative controls (94.5 ± 6.4 *vs.* 71.7 ± 5.3 mL/min/100 g, and 28.0% ± 1.6% *vs.* 21.6% ± 1.0%), stem cell-hydrogel PF and degenerative controls (86.1 ± 6.9 *vs.* 71.7 ± 5.33 mL/min/100 g, 26.3% ± 1.2% *vs.* 21.6% ± 1.0%), and hydrogel PF and HA compared with normal controls. No difference between hydrogel PF and HA compared to degenerative controls or normal control *versus* stem cell-hydrogel PF was found. Data are summarized in Table 1.

In permeability parameters, statistical difference was found when normal and degenerative controls (1.1 ± 0.1 *vs.* 0.7 ±

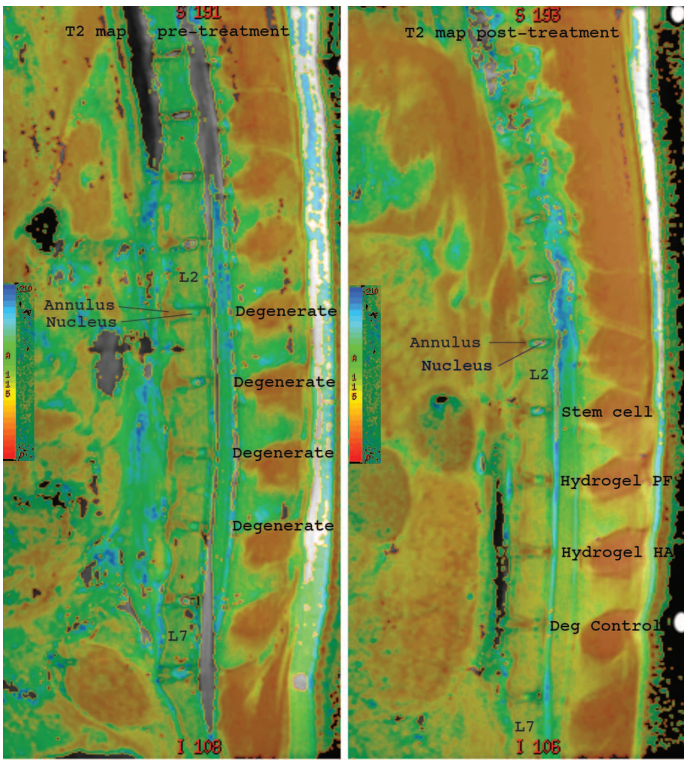

Figure 3. Representative color-coded T2 maps. Left side is before intervention, while right side is 12 weeks posttreatment. Blue is high T2 relaxation time, whereas red is low T2. Color-coded bars are shown to the left in each image.

0.1; $P < 0.0001$) were compared, and between stem cell-hydrogel PF *versus* degenerative controls (1.0 ± 0.1 *vs.* 0.7 ± 0.1; $P < 0.0001$). Data are summarized in Table 1.

The avascular disc spaces were black in both perfusion and permeability maps. This is due to the lack of gadolinium in the disc and subsequently no change in signal intensity. Representative maps (rBF, rBV, and permeability) are shown in Figure 4 and data are summarized in Figure 4.

In postcontrast (45 minutes) T1-weighted MRI, significant differences were found between normal and degenerative controls (64.5 ± 5.2 *vs.* 33.0 ± 2.9; $P < 0.0001$) and stem cell-hydrogel PF and degenerative controls (59.9 ± 3.1; $P < 0.0001$), but not in any other comparisons as with rBF, rBV, and T2 mapping data. Data are displayed in Table 1.

Generally normal controls exhibited a hyperintense zone in the upper and lower parts of the NP adjacent to endplates. No enhancement was found in the central NP. No tears of the posterior annulus fibrosus were seen and no neovascularization (high-intensity bands running from the endplate into the NP) was detected. Stem cell-hydrogel PF levels had slightly lower but still visible intensity bands compared to normal controls. In hydrogel PF, hydrogel HA, and degenerative control levels, no clear bands of the peripheral NP could be visualized.

A weak but statistically significant correlation was established between permeability and enhancement percentage ($R = 0.42$ and $P = 0.039$). Pre- and postcontrast enhanced images are shown in Figure 5.

DISCUSSION

IDD is multifactorial with influence from various factors such as genetic inheritance,[19–21] ageing,[22] decreased nutrition,[23–26] mechanical overload.[27–30] Even though IDD is multifactorial, decreased nutrition and structural changes affecting morphology and function of the intervertebral disc are thought to be major important pathways in IDD.

The endplate is a crucial part of the mechanical properties and in nutrition of the intervertebral disc. The endplate is subjected to microcracks and damage from infancy progressing through life.[31]

MRI has become the gold standard for assessment of the intervertebral disc. The discs itself consisting of annulus fibrosus and NP are clearly visualized by MRI with classification algorithms.[18,32] de Roos *et al*[33] and Modic *et al*[34] have described three types of endplate changes. However, these changes appear in the marrow and subchondral bone.

Recently, a grading system on the basis of serial postcontrast MRI was proposed by Rajasekaran *et al*.[11] The same technique has been used previously in experimental IDD[35]

TABLE 1. Data Summarized for T2 Relaxation Time, Pfirrmann Grade, Relative Blood Flow, Relative Blood Volume, Permeability, and T1 Contrast Enhancement Percentage

	Normal Control	Degenerate Control	Stem Cell—Hydrogel	Hydrogel PF	Hydrogel HA
T2 time (ms)	94.4 ± 5.4	61.7 ± 5.9	87.6 ± 5.9	73.1 ± 5.4	68.9 ± 4.6
Pfirrmann	1 ± 0	3.5 ± 0.7	2.1 ± 0.3	2.8 ± 0.6	2.9 ± 0.7
rBF (mL/min/100 g)	94.5 ± 6.4	71.7 ± 5.3	86.1 ± 6.9	78.5 ± 7.4	76.4 ± 6.3
rBV (%)	28.0 ± 1.6	21.6 ± 1.0	26.3 ± 1.2	23.0 ± 1.2	22.6 ± 1.4
Permeability	1.1 ± 0.1	0.7 ± 0.1	1.0 ± 0.1	0.8 ± 0.1	0.8 ± 0.1
Contrast enhancement (%)	64.5 ± 5.2	33.0 ± 2.9	59.9 ± 3.1	47.7 ± 4.6	45.4 ± 6.6

Data are given as mean ± standard deviation.
rBF indicates relative blood flow; rBV, relative blood volume.

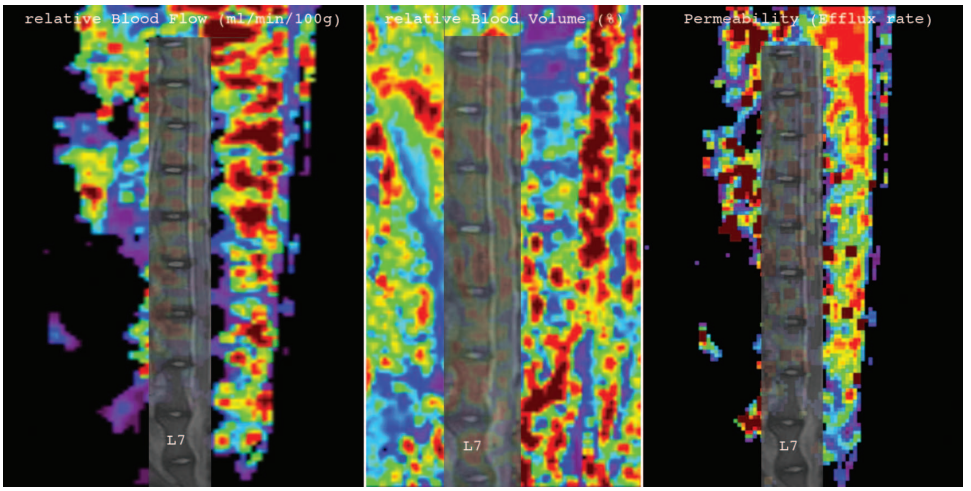

Figure 4. Representative color-coded maps of rBF (mL/min/100 g), relative blood volume (%), and permeability. Black spots are the intervertebral discs, where no signal change appear because of avascularity. A T2-weighted midsagittal image has been overlaid. Nucleus pulposus is seen white in the black spots in the functional maps with surrounding vertebrae.

and quantitated in healthy volunteers.[36] Serial postcontrast MRI requires several MRIs of the patient separated by at least 2 hours between scans. Furthermore, the activity between serial scans has to follow a protocol because rest and physical activity alters fluid flow in and out of the intervertebral disc and with this contrast agent. This can be achieved in patients suffering from osteoarthritis where dGEMRIC (delayed Gadolinium Enhanced MRI of Cartilage) is used in the evaluation of cartilage[37] but can be troublesome in patients with IDD, neurogenic claudication, LBP, *etc*. When this is said, serial postcontrast MRI currently provides reliable noninvasive data on endplate function with regard to disc nutrition.

This study investigated flow and permeability parameters by DCE-MRI in regeneration of experimental IDD. Significant differences were found in stem cell-hydrogel PF-treated discs with regard to rBF and blood volume as well as permeability and postcontrast enhancement compared to degenerative controls.

Pfirrmann grades and T2 mapping confirmed a regenerative capacity of stem cells-hydrogel PF when focusing on the NP. T2 values obtained correspond well to the data published on normal and degenerate human intervertebral discs, with Pfirrmann grade 2 discs having T2 values of 87.617 and 85 milliseconds and grades 3 to 4 discs having T2 values of 61.692 and 53 milliseconds, respectively.[38]

There was no statistical difference between hydrogel only-treatment and degenerative controls; however, all imaging methods gave an impression of slight improvement. These results are supported by Hohaus *et al*,[39] who found stem cell and hyaluronic acid superior to hyaluronic acid in a dog study.

Only weak correlation between DCE-MRI permeability and postcontrast enhancement was established. There may be several reasons for this. First, DCE-MRI measure flux of contrast in a two-compartmental model—from the intravascular space to the extravascular space and *vice versa*. Permeability quantitates vascular permeability and not the flux of contrast through the endplate. Blood flow *etc*. is not an entirely passive process in the vertebra. Muscarinic receptors have been found indirectly in the vasculature, and blood flow is regulated by humoral factors.[40] On the contrary, inhibition of endplate perfusion results in decreased diffusion through the vertebral endplate.[41]

Second, the DCE-MRI sequence was a low-resolution sequence with resolution of 128 × 128. Newer sequences offer resolution of 256 × 256 with better anatomic imaging and four times higher spatial resolution still at 1.5 T. The spatial resolution decreases, but this is of minor importance.[13] With the advancement of 3-T whole-body scanners, resolution and anatomy improve. In this study, manual injection of 0.1 mmol/kg contrast was used. Automated injection would provide more stable contrast delivery; however, this should be of no importance as the study is paired. Increasing the amount of contrast injected intravenously would increase contrast between vasculature and extravascular space. However, the value of this remains unknown.

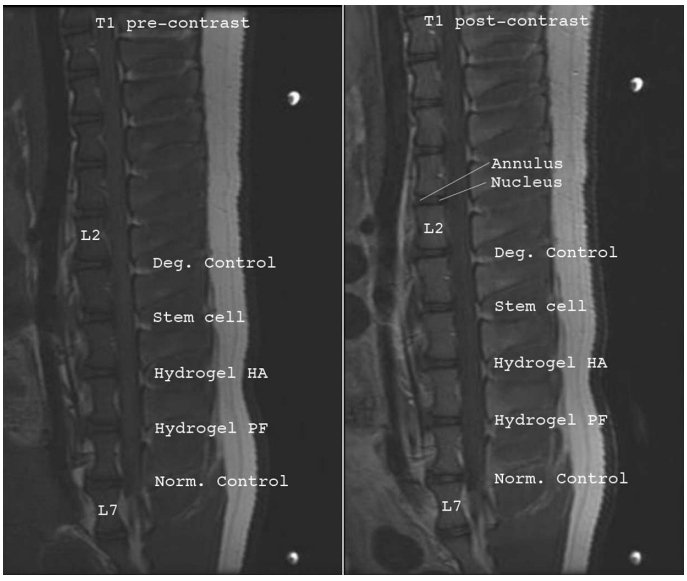

Figure 5. Representative T1 images before and 45 minutes after intravenous gadolinium injection. Left-side image is precontrast and right-side image is postcontrast. Mesenchymal stem cell–treated levels exhibit good enhancement in the peripheral nucleus pulposus as with normal controls. Degenerate controls have diminished enhancement with slight irregularity. Hydrogels alone have some regular enhancement.

Relative BV gives an indirect measure of percentage of vasculature in a given volume of interest. This could be an interesting parameter in regenerative studies but needs correlation to endplate vascularity by, for instance, immunohistomorphometry

Skeletally mature Gottingen minipigs were used. The minipig maintains an open epiphysis though fully grown. Furthermore, notochordal cells are present but disappear in induced IDD (unpublished data). Relevance of quadruped models of IDD is often questioned. Most quadruped spines have to sustain substantial bending forces due to the abdomen. Spinal alignment is maintained by counteracting forces exerted by the multifidus. As a consequence, the quadruped spine is loaded by axial compression as with the human spine. Animals have a higher vertebral bone density, suggesting higher axial compression forces.[42] Moreover, the principal direction of vertebral trabeculae is in the craniocaudal direction (M. Bendtsen, PhD thesis 2009; University of Aarhus, Denmark).

Quadrupeds walk asymmetrically with at least one foot off the ground during the walking cycle. This implies that the thorax and pelvis are affected by opposite torsion moments with axial rotation in the lumbar spine[42] and torsional stiffness similar to humans.[43,44]

Even though the Gottingen minipig is considered a large animal model of IDD, disc height does not reach the same as in humans. At approximately 4 mm, it is still sufficient to make diffusion of nutrients an issue in biologic therapy for IDD.

Stem cells dissolved in a hydrogel were able to maintain blood flow, volume, and permeability of vertebral endplates and subchondral bone for a period of 3 months. IDD was of moderate grade at the time of intervention.

The mechanism of endplate "protection" remains unknown, whether it is a biomechanical factor with appropriate loading of the central endplate or biochemical factors secreted from transplanted MSCs or native NP cells, or a combination needs further clarification.

Generally, there is consensus that there is a "point of no return" in IDD in which biologic therapy will fail because of severity of biomechanical changes and limitation of nutritional supply.

This study does not address the appropriate grade for stem cell therapy or the optimal amount of transplantation or which cell type is the most suitable for regeneration of IDD. These are all unanswered questions that need to be addressed before cell-based therapy can be considered a clinical option in the treatment of IDD; long-term studies on the effect of biologic therapy on the endplate are also warranted.

CONCLUSION

DCE-MRI quantitates blood flow, volume, and vascular permeability in the vertebral endplate and subchondral bone. A weak correlation between vascular permeability and postcontrast enhancement was established.

DCE-MRI, using high-resolution sequences, may become an important tool in the evaluation of endplate function and thus decision making in future biologic therapy but needs verification.

Autologous stem cell-hydrogel therapy, in contrast to hydrogel alone, is able to induce a regenerative response and maintain the function of the vertebral endplate in a porcine model with 3 months' follow-up.

➢ Key Points

- ❑ Autologous stem cell therapy is able to regenerate the NP in intervertebral disc degeneration to some extent.
- ❑ Dynamic contrast-enhanced MRI assesses function of the vertebral endplate and might replace serial T1 postcontrast MRI
- ❑ Autologous stem cell therapy protects the function of the vertebral endplate in IDD.
- ❑ Autologous stem cells are able to survive at least 12 weeks *in vivo* when subjected to the environment in disc degeneration.

References

1. Anderson GB. Epidemiological factors of chronic low-back pain. *Lancet* 1999;354:581–5.
2. Adams MA, Roughley PJ. What is intervertebral disc degeneration, and what causes it? *Spine* 2006;31:2151–61.
3. Grunhagen T, Wilde G, Soukane DM, et al. Nutrient supply and intervertebral disc metabolism. *J Bone Joint Surg Am* 2006;88(suppl 2): 30–5.
4. Natarajan RN, Ke JH, Anderson GB. A model to study the disc degeneration process. *Spine* 1994;19:259–65.
5. Moore RJ, Vernon-Roberts B, Fraser RD, et al. The origin of and fate of herniated lumbar intervertebral tissue. *Spine* 1996;21: 2149–55.
6. Rajasekaran S, Naresh BJ, Arun R, et al. ISSLS Prize Winner. A study of diffusion in human lumbar discs. *Spine* 2004;29: 2654–67.
7. Benneker LM, Heini PF, Alini M, et al. 2004 young Investigator Award Winner: vertebral end-plate marrow contact channel occlusions and intervertebral disc degeneration. *Spine* 2005;30:167–73.
8. Gruber HE, Ashraf N, Kilburn J, et al. Vertebral endplate architecture and vascularization: application of micro-computed tomography, a vascular tracer and immunohistochemistry in analysis of disc degeneration in the aging sand rat. *Spine* 2005;30:2593–600.
9. Buckwalter JA. Aging and degeneration of the human intervertebral disc. *Spine* 1995;20:1307–14.
10. Nerlich AG, Schleicher E, Boos N. 1997 Volvo Award Winner in basic science studies. Immunohistologic markers for age-related changes of human lumbar intervertebral discs. *Spine* 1995;22: 2781–95.
11. Rajasekaran S, Venkatadass K, Babu JN, et al. Pharmacological enhancement of disc diffusion and differentiation of healthy, ageing and degenerated discs. Results from *in-vivo* serial post-contrast MRI studies in 365 human lumbar discs. *Eur Spine J* 2008;17: 626–43.
12. Griffith JF, Yeung DK, Antonio GE, et al. Vertebral bone mineral density, marrow perfusion and fat content in healthy men and men with osteoporosis. Dynamic contrast-enhanced MR imaging and MR spectroscopy. *Radiology* 2005;236:945–51.
13. Libicher M, Kasperk C, Daniels M, et al. Dynamic contrast-enhanced MRI in Paget's disease of bone—correlation of regional microcirculation and bone turnover. *Eur Radiol* 2008;18:1005–11.
14. Yin JJ, Tracy K, Zhang L, et al. Noninvasive imaging of the functional effects of anti-VEGF therapy on tumor cell extravasation and regional blood volume in an experimental brain metastasis model. *Clin Exp Metastasis* 2009;26:403–14.

15. Veeravagu A, Hou LC, Hsu AR, et al. The temporal correlation of dynamic contrast-enhanced magnetic resonance imaging with tumor angiogenesis in a murine glioblastoma model. *Neurol Res* 2008;30:952–9.
16. Roberts S, Evans EH, Kletsas D, et al. Senescence in human intervertebral discs. *Eur Spine J* 2006;15:3112–6.
17. Gruber HE, Ingram JA, Norton HJ, et al. Senescence in cells of the aging and degenerating intervertebral discs: immunolocalization of senescence-associated beta-galactosidase in human and sand rat discs. *Spine* 2007;32:321–7.
18. Pfirrmann CW, Metzdorf A, Elfering A, et al. Effect of aging and degeneration on disc volume and shape: a quantitative study in asymptomatic volunteers. *J Orthop Res* 2006; 1086–94.
19. Annunen J, Paassilta P, Lohiniva J, et al. An allele of COL9A2 associated with intervertebral disc disease. *Science* 1999;285:409–12.
20. Takahashi M, Haro H, Wakabayashi Y, et al. The association of degeneration of the intervertebral disc with 5a/6a polymorphism in the promoter of the human matrix metalloproteinase-3 gene. *J Bone Joint Surg Br* 2001;83:491–5.
21. Videman T, Saarela J, Kaprio J, et al. Association of 25 structural degradative, and inflammatory candidate genes with lumbar disc desiccation, bulging, and height narrowing. *Arthritis Rheum* 2009;60:470–81.
22. Adams MA, Roughley PJ, Buckwalter JA. Spine update: ageing and degeneration of the human intervertebral disc. *Spine* 1995;20: 1307–14.
23. Gruber HE, Hanley EN Jr. Recent advances in disc cell biology. *Spine* 2003;28:186–93.
24. Roberts S, Menage J, Urban JP. Biochemical and structural properties of the cartilage end-plate and its relation to the intervertebral disc. *Spine* 1989;14:166–74.
25. Stairman JW, Holm S, Urban JP. Factors influencing oxygen concentration gradients in the intervertebral disc: a theoretical analysis. *Spine* 1991;16:444–9.
26. Urban JP, Holm S, Maroudas A. Diffusion of small solutes into the intervertebral disc: an *in vivo* study. *Biorheology* 1978;15:203–21.
27. Adams MA, Freeman BJ, Morrison HP, et al. Mechanical initiation of intervertebral disc degeneration. *Spine* 2000;25:1625–36.
28. Hutton WC, Elmer WA, Boden SD, et al. The effect of hydrostatic pressure on intervertebral disc metabolism. *Spine* 1999;24:1507–15.
29. Lotz JC, Chin JR. Intervertebral disc cell death is dependent on the magnitude and duration of spinal loading. *Spine* 2000;25:1477–82.
30. Walsh AJ, Lotz JC. Biological response of the intervertebral disc to dynamic loading. *J Biochem* 2004;37:329–37.
31. Boos N, Weissbach S, Rohrbach H, et al. 2002 Volvo Award in Basic Science: classification of age-related changes in lumbar intervertebral discs. *Spine* 2002;27:2631–44.
32. Osti OL, Vernon-Roberts B, Moore R, et al. Annular tears and disc degeneration in the lumbar spine. A post mortem study of 135 discs. *J Bone Joint Surg* 1992;74:678–82.
33. de Roos A, Kressel H, Spritzer C, et al. MR imaging of marrow changes adjacent to end plates in degenerative lumbar disk disease. *Am J Roentgenol* 1987;149:531–4.
34. Modic MT, Steinberg PM, Ross JS, et al. Degenerative disc disease: assessment of changes in vertebral body marrow with MR imaging. *Radiology* 1988;166:193–9.
35. Nguyen-minh C, Ho K-C, Xu R, et al. Effect of degeneration of the intervertebral disk on the process of diffusion. *Am J Neuroradiol* 1997;18:435–42.
36. Niinimäki JL, Parviainen O, Ruohonen J, et al. *In vivo* quantification of delayed gadolinium enhancement in the nucleus pulposus of human intervertebral disc. *J Magn Reson Imaging* 2006;24: 796–800.
37. Multanen J, Rauvala E, Lammentausta E, et al. Reproducibility of imaging human knee cartilage by delayed gadolinium-enhanced MRI of cartilage (dGEMRIC) at 1.5 Tesla. *Osteoarthritis Cartilage* 2009;17:559–64.
38. Perry J, Haughton V, Anderson PA, et al. The value of T2 relaxation times to characterize lumbar intervertebral disks: preliminary results. *Am J Neuroradiol* 2006;27:337–42.
39. Hohaus C, Ganey TM, Minnkus Y, et al. Cell transplantation in lumbar spine disc degeneration disease. *Eur Spine J* 2008;17(suppl 4): 492–503.
40. Wallace A, Wyatt BC, McCarthy ID, et al. Humoral regulation of blood flow in the vertebral endplate. *Spine* 1994;19:1324–8.
41. Werf MV, Lezuo P, Maissen O, et al. Inhibition of vertebral endplate perfusion results in decreased intervertebral disc intranuclear diffusive transport. *J Anat* 2007;211:769–74.
42. Smit TH. The use of quadrupeds as an *in vivo* model for the study of the spine—biomechanical considerations. *Eur Spine J* 2002;1:137–44.
43. Wilke HJ, Krischak S, Claes L. Biomechanical comparison of calf and human spines. *J Orthop Res* 1996;14:500–3.
44. Wilke HJ, Kettler A, Claes L. Are sheep spines a valid model for human spines. *Spine* 1997;22:2365–74.